Wood Science and Technology 32 (1998) 325–334 © Springer-Verlag 1998

A numerical study of the shape stability of sawn timber subjected to moisture variation

Part 1: Theory

S. Ormarsson, O. Dahlblom, H. Petersson

Abstract A three-dimensional theory for the numerical simulation of deformations and stresses in wood during moisture variation is described. The constitutive model employed, assumes the total strain rate to be the sum of the elastic strain rate, the moisture-induced strain rate and the mechano-sorption strain rate. Wood is assumed to be an orthotropic material with large differences between the longitudinal, radial and tangential directions in the properties found. The influence of the growth rings, the spiral grain and the conical shape of the log on the orthotropic directions in the wood is taken account of in the model. A finite element formulation is used to describe the deformation process and the stress development during drying.

Introduction

In timber exposed to moisture variations, deformations as cup, twist, crook and bow (see Fig. 1), is a serious problem since it can make the wood products unsuitable for construction purposes cf. (Johansson et al. 1994 and Perstorper et al. 1995). To improve the shape stability of such products, it is important to clarify how the properties of the material, its internal structure and environmental conditions affect the deformation process. However, the complex behaviour of wood makes computer simulation necessary. Theoretical simulation of the deformation process requires a proper constitutive model. It is important that such a model take account both of the direction dependence of the material and of the behaviour of wood being strongly influenced by variations in moisture content. The internal structure of wood allows it to be defined locally as being an orthotropic material. In the description that follows, an orthotropic coordinate system will be used as a local coordinate system. The coordinate system is de-

Received 24 April 1997

S. Ormarsson, O. Dahlblom
Division of Structural Mechanics, Lund Institute of Technology,
Lund University, Box 118, SE-221 00 Lund, Sweden

H. Petersson
Department of Structural Mechanics,
Chalmers University of Technology,
SE-412 96 Göteborg, Sweden

The research presented in this paper is a part of the national research programme in Sweden concerning wood physics and drying. It was financially supported by the Research Foundation of Swedish Sawmills and the Swedish Council for Forestry and Agricultural Research.

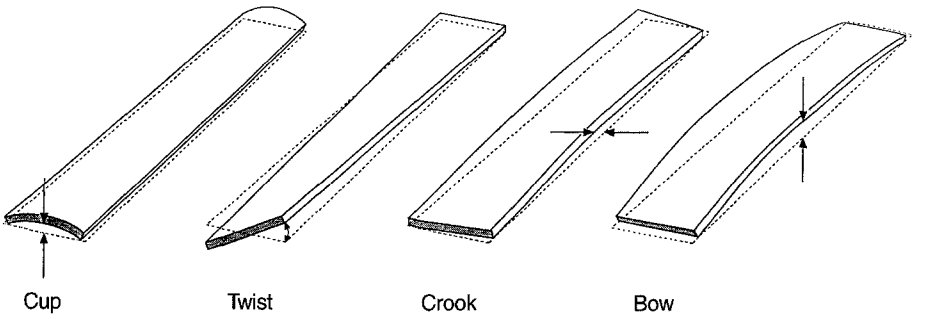

Fig. 1. The various deformation types

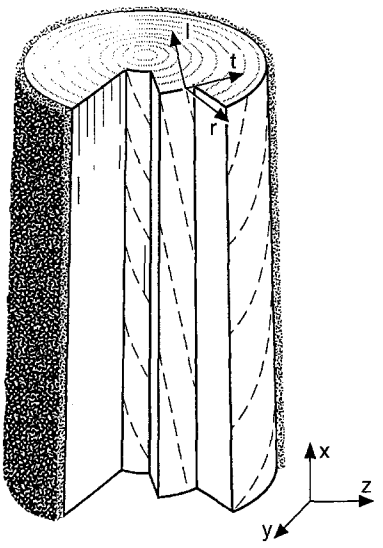

Fig. 2. Global and local coordinate system

noted by the letters l, r and t, which designate the longitudinal, radial and tangential directions in the wood material, see Fig. 2. Variables with a bar relate to this local coordinate system, while variables without a bar relate to a global coordinate system x, y, z.

Modelling of strain

The total strain rate $\dot{\bar{\varepsilon}}$ is assumed to be the sum of the elastic strain rate $\dot{\bar{\varepsilon}}_e$, the moisture strain rate $\dot{\bar{\varepsilon}}_w$ and the mechano-sorptive strain rate $\dot{\bar{\varepsilon}}_{w\sigma}$, i.e.

$$\dot{\bar{\varepsilon}} = \dot{\bar{\varepsilon}}_e + \dot{\bar{\varepsilon}}_w + \dot{\bar{\varepsilon}}_{w\sigma} \tag{1}$$

This means that neither creep nor the influence of cracking is considered.

Elastic strain

Elastic strain is related to stress by Hooke's law

$$\bar{\varepsilon}_e = \bar{C}\bar{\sigma} \tag{2}$$

where $\bar{C}$ is the compliance matrix and $\bar{\varepsilon}_e$ and $\bar{\sigma}$ denote elastic strain and stress, respectively. The elastic strain rate $\dot{\bar{\varepsilon}}_e$ is obtained by differentiation of Eq. (2):

$$\dot{\bar{\varepsilon}}_e = \bar{C}\dot{\bar{\sigma}} + \dot{\bar{C}}\bar{\sigma} \tag{3}$$

where a dot denotes the derivative with respect to time. The vectors $\bar{\varepsilon}_e$, $\bar{\sigma}$ and the matrix $\bar{C}$ are as follows:

$$\bar{\varepsilon}_e = [\varepsilon_l \ \varepsilon_r \ \varepsilon_t \ \gamma_{lr} \ \gamma_{lt} \ \gamma_{rt}]^T \tag{4}$$

$$\bar{\sigma} = [\sigma_l \ \sigma_r \ \sigma_t \ \tau_{lr} \ \tau_{lt} \ \tau_{rt}]^T \tag{5}$$

$$\bar{C} = \begin{bmatrix} \frac{1}{E_l} & -\frac{\nu_{rl}}{E_r} & -\frac{\nu_{tl}}{E_t} & 0 & 0 & 0 \\ -\frac{\nu_{lr}}{E_l} & \frac{1}{E_r} & -\frac{\nu_{tr}}{E_t} & 0 & 0 & 0 \\ -\frac{\nu_{lt}}{E_l} & -\frac{\nu_{rt}}{E_r} & \frac{1}{E_t} & 0 & 0 & 0 \\ 0 & 0 & 0 & \frac{1}{G_{lr}} & 0 & 0 \\ 0 & 0 & 0 & 0 & \frac{1}{G_{lt}} & 0 \\ 0 & 0 & 0 & 0 & 0 & \frac{1}{G_{rt}} \end{bmatrix} \tag{6}$$

The parameters E_l, E_r, E_t are the moduli of elasticity in the orthotropic directions and G_{lr}, G_{lt}, G_{rt} are the shear moduli in the respective orthotropic planes. The parameters ν_{lr}, ν_{rl}, ν_{lt}, ν_{tl}, ν_{rt} and ν_{tr} are Poisson's ratios. Since the compliance matrix $\bar{C}$ is assumed to be symmetric, the Poisson's ratios are related as follows: $\nu_{rl} = \frac{E_r}{E_l}\nu_{lr}$, $\nu_{tl} = \frac{E_t}{E_l}\nu_{lt}$ and $\nu_{tr} = \frac{E_t}{E_r}\nu_{rt}$.

The moduli E_l, E_r, E_t and G_{lr}, G_{lt}, G_{rt} depend on moisture content and temperature, see e.g. (Dinwoodie 1981). If the moisture content is higher than the fibre saturation point w_f, variation in moisture content is assumed to have no influence on the moduli. In the present study the elastic and shear moduli are assumed to be given by

$$E_l = E_{l0}(1 + E_{lT}(T_0 - T)) + E_{lw}(w_f - w_a) \tag{7}$$

$$E_r = E_{r0}(1 + E_{rT}(T_0 - T)) + E_{rw}(w_f - w_a) \tag{8}$$

$$E_t = E_{t0}(1 + E_{tT}(T_0 - T)) + E_{tw}(w_f - w_a) \tag{9}$$

$$G_{lr} = G_{lr0}(1 + G_{lrT}(T_0 - T)) + G_{lrw}(w_f - w_a) \tag{10}$$

$$G_{lt} = G_{lt0}(1 + G_{ltT}(T_0 - T)) + G_{ltw}(w_f - w_a) \tag{11}$$

$$G_{rt} = G_{rt0}(1 + G_{rtT}(T_0 - T)) + G_{rtw}(w_f - w_a) \tag{12}$$

where

$$w_a = w \qquad \text{if} \quad w \leq w_f \tag{13}$$

$$w_a = w_f \qquad \text{if} \quad w > w_f \tag{14}$$

The parameters E_{l0}, E_{r0}, E_{t0}, G_{lr0}, G_{lt0} and G_{rt0} are the basic values of the moduli at temperature $T = T_0 = 20\ ^\circ C$ and with the moisture content w being equal to or higher than the fibre saturation point w_f. The quantities E_{lw}, E_{rw}, E_{tw}, G_{lrw}, G_{ltw}, G_{rtw}, E_{lT}, E_{rT}, E_{tT}, G_{lrT}, G_{ltT} and G_{rtT} are material parameters describing the influence of moisture content and temperature. In wood, the moisture content w is defined as

$$w = \frac{w_w}{w_0} \tag{15}$$

where w_w is the weight of the water in a wood sample and w_0 is the oven-dry weight of the same sample.

The fibre saturation point w_f is defined as the amount of water required for saturation of the cell wall, without the presence of any free water in the cell lumen. This point is dependent on temperature T, see e.g. (Bodig and Jayne 1982), and is assumed here to be

$$w_f = w_{f0}(1 + w_{fT}(T_0 - T)) \tag{16}$$

where w_{f0} is the basic fibre saturation point at temperature $T = T_0$. The parameter w_{fT} describes the influence of temperature on the fibre saturation point.

Moisture-induced strain

Changes in moisture content are accompanied by considerable shrinkage or swelling of the material, see e.g. (Kollmann and Côté 1968). The moisture-induced strain rate is assumed to depend solely upon the rate of change in moisture content. It is defined as

$$\dot{\bar{\varepsilon}}_w = \boldsymbol{\alpha}\dot{w}_a \tag{17}$$

where $\dot{w}_a$ denotes the rate of change in moisture content below the fibre saturation point. The matrix $\boldsymbol{\alpha}$ is defined as

$$\boldsymbol{\alpha} = [\alpha_l \; \alpha_r \; \alpha_t \; 0 \; 0 \; 0]^T \tag{18}$$

The parameters α_l, α_r and α_t are material coefficients of moisture-induced strain in the three orthotropic directions. Although that the shrinkage parameters may be dependent on temperature and on moisture content, this is not taken into account here due to the lack of experimental data.

Mechano-sorptive strain

If a wood specimen under load is allowed to dry, it exhibits greater deformation than the sum of the deformation of a loaded specimen under constant humidity condition and the deformation of a non-loaded drying specimen. This phenomenon, termed the mechano-sorptive effect, can be expressed, see (Ranta-Maunus 1990, Santaoja et al. 1991 and Thelandersson and Morén 1990), as follows:

$$\dot{\bar{\varepsilon}}_{w\sigma} = \bar{\mathbf{m}}\bar{\boldsymbol{\sigma}}|\dot{w}_a| \tag{19}$$

In Eq. (19), $|\dot{w}_a|$ denotes the absolute value of the rate of change in moisture content below the fibre saturation point. The matrix $\bar{\boldsymbol{\sigma}}$ is the stress matrix and $\bar{\mathbf{m}}$ the mechano-sorption property matrix, the latter defined as

$$\bar{\mathbf{m}} = \begin{bmatrix} m_l & -\mu_{rl}m_r & -\mu_{tl}m_t & 0 & 0 & 0 \\ -\mu_{lr}m_l & m_r & -\mu_{tr}m_t & 0 & 0 & 0 \\ -\mu_{lt}m_l & -\mu_{rt}m_r & m_t & 0 & 0 & 0 \\ 0 & 0 & 0 & m_{lr} & 0 & 0 \\ 0 & 0 & 0 & 0 & m_{lt} & 0 \\ 0 & 0 & 0 & 0 & 0 & m_{rt} \end{bmatrix} \tag{20}$$

where m_l, m_r, m_t, m_{lr}, m_{lt} and m_{rt} are mechano-sorption coefficients for the orthotropic directions and for the orthotropic planes. The coefficients μ_{lr}, μ_{lt}, μ_{rt}, μ_{rl}, μ_{tl} and μ_{tr} describe the coupling of the mechano-sorptive strain between the different directions. The mechano-sorption matrix is assumed to be symmetric, resulting in the relations $\mu_{rl} = \frac{m_l}{m_r}\mu_{lr}$, $\mu_{tl} = \frac{m_l}{m_t}\mu_{lt}$ and $\mu_{tr} = \frac{m_r}{m_t}\mu_{rt}$. According to (Carlsson and Thunell 1975 and Castera 1989), mechano-sorption is dependent on temperature. The parameters m_l, m_r, m_t, m_{lr}, m_{lt} and m_{rt} are thus assumed, very simply, to be

$$m_l = m_{l0}(1 + m_{lT}(T_0 - T)) \tag{21}$$

$$m_r = m_{r0}(1 + m_{rT}(T_0 - T)) \tag{22}$$

$$m_t = m_{t0}(1 + m_{tT}(T_0 - T)) \tag{23}$$

$$m_{lr} = m_{lr0}(1 + m_{lrT}(T_0 - T)) \tag{24}$$

$$m_{lt} = m_{lt0}(1 + m_{ltT}(T_0 - T)) \tag{25}$$

$$m_{rt} = m_{rt0}(1 + m_{rtT}(T_0 - T)) \tag{26}$$

The parameters m_{l0}, m_{r0}, m_{t0}, m_{lr0}, m_{lt0} and m_{rt0} are the material parameters at temperature $T = T_0 = 20\ ^\circ C$. The coefficients m_{lT}, m_{rT}, m_{tT}, m_{lrT}, m_{ltT} and m_{rtT} describe the influence of temperature.

Global material formulation

The total strain rate in Eq. (1) is expressed in terms of a local coordinate system. According to Eq. (3), the stress rate in the local system can be expressed as

$$\dot{\bar{\sigma}} = \bar{D}(\dot{\bar{\varepsilon}}_e - \dot{\bar{C}}\bar{\sigma}) \tag{27}$$

where the matrix $\bar{D}$ is the inverse of the local compliance matrix $\bar{C}$ shown in Eq. (6). Substitution of Eq. (1) into Eq. (27) yields

$$\dot{\bar{\sigma}} = \bar{D}\dot{\bar{\varepsilon}} - \dot{\bar{\sigma}}_0 \tag{28}$$

where $\dot{\bar{\sigma}}_0$ is a so-called pseudo-stress vector describing the effect of moisture change. The vector is given by

$$\dot{\bar{\sigma}}_0 = \bar{D}(\dot{\bar{\varepsilon}}_w + \dot{\bar{\varepsilon}}_{\sigma w} + \dot{\bar{C}}\bar{\sigma}) \tag{29}$$

Substitution of Eqs. (17) and (19) into Eq. (29) yields

$$\dot{\bar{\sigma}}_0 = \bar{D}(\boldsymbol{\alpha}\dot{w}_a + \bar{\mathbf{m}}\bar{\sigma}|\dot{w}_a| + \dot{\bar{C}}\bar{\sigma}) \tag{30}$$

The relation (28) above refers to the local coordinate system (**l, r, t**). This has to be transformed to the global coordinate system (**x, y, z**) see Fig. 2, if account is to be taken of variation in the orthotropic directions due to annual rings, spiral grain and conicity. This transformation is performed in three steps.

The first step is to establish the relation between the global directions and a system of coordinates having its origin at the surface of a circular cylinder and its central axis along the pith. In this system, the axis $\mathbf{l}_0$ is parallel to the pith, $\mathbf{r}_0$ is perpendicular to the surface of the cylinder and $\mathbf{t}_0$ is tangential to the surface of the cylinder. Fig. 3 indicates the vectors used in the formulation that follows.

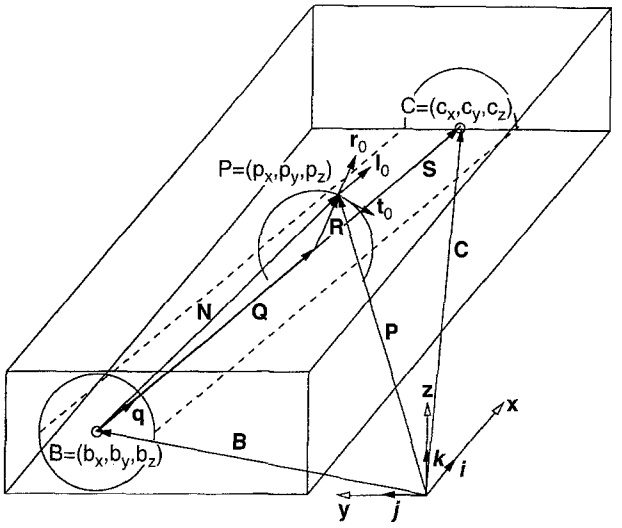

Fig. 3. Geometry of the vectors used in calculating the direction cosines between the global and the local coordinate-axes

The material point P has the coordinates (p_x, p_y, p_z), the points B and C on the pith being assumed to have the coordinates (b_x, b_y, b_z) and (c_x, c_y, c_z), respectively. On the basis of these assumptions, the relation between the axes $\mathbf{l}_0$, $\mathbf{r}_0$ and $\mathbf{t}_0$ and the global axes **i**, **j** and **k** can be determined. The vector **P** from the origin to the material point P, the vector **B** from the origin to point B and the vector **C** from the origin to point C are defined as

$$\mathbf{P} = p_x\mathbf{i} + p_y\mathbf{j} + p_z\mathbf{k} \tag{31}$$

$$\mathbf{B} = b_x\mathbf{i} + b_y\mathbf{j} + b_z\mathbf{k} \tag{32}$$

$$\mathbf{C} = c_x\mathbf{i} + c_y\mathbf{j} + c_z\mathbf{k} \tag{33}$$

The vector **N** from point B to point P and the vector **S** in the pith direction, from the base to the top of the tree, are defined by

$$\mathbf{N} = \mathbf{P} - \mathbf{B} \tag{34}$$

$$\mathbf{S} = \mathbf{C} - \mathbf{B} \tag{35}$$

The unit vector **q** in the pith direction is given by

$$\mathbf{q} = \frac{\mathbf{S}}{|\mathbf{S}|} \tag{36}$$

The vector **Q** is a projection of the vector **N** on the pith direction, i.e.

$$\mathbf{Q} = (\mathbf{N} \cdot \mathbf{q})\mathbf{q} \tag{37}$$

The vector **R** perpendicular to both the pith and the surface of the cylinder is given by

$$\mathbf{R} = \mathbf{N} - \mathbf{Q} \tag{38}$$

The unit vectors $\mathbf{l}_0$, $\mathbf{r}_0$, and $\mathbf{t}_0$ can then be calculated as

$$\mathbf{l}_0 = \mathbf{q} \tag{39}$$

$$\mathbf{r}_0 = \frac{\mathbf{R}}{|\mathbf{R}|} \tag{40}$$

$$\mathbf{t}_0 = \mathbf{l}_0 \times \mathbf{r}_0 \tag{41}$$

These directions coincide with the orthotropic directions in the wood, provided no conical effect or spiral grain is present at the material point studied. The nine direction cosines defining the relation between the local and global coordinate systems can be written in matrix form as

$$\begin{bmatrix} \mathbf{l}_0 \\ \mathbf{r}_0 \\ \mathbf{t}_0 \end{bmatrix} = \mathbf{A}_0^{\mathrm{T}} \begin{bmatrix} \mathbf{i} \\ \mathbf{j} \\ \mathbf{k} \end{bmatrix} \tag{42}$$

where

$$\mathbf{A}_0 = \begin{bmatrix} a^x_{l_0} & a^x_{r_0} & a^x_{t_0} \\ a^y_{l_0} & a^y_{r_0} & a^y_{t_0} \\ a^z_{l_0} & a^z_{r_0} & a^z_{t_0} \end{bmatrix} = \begin{bmatrix} l_{0x} & r_{0x} & t_{0x} \\ l_{0y} & r_{0y} & t_{0y} \\ l_{0z} & r_{0z} & t_{0z} \end{bmatrix} \tag{43}$$

where l_{0x}, r_{0x}, t_{0x} etc. are the vector components of the respective unit vectors $\mathbf{l}_0$, $\mathbf{r}_0$ and $\mathbf{t}_0$.

The second step in the transformation is to take account of the effect of the conical angle ϕ, see Fig. 4. The coordinate rotation due to the conical angle is shown in Fig. 4. The conical angle ϕ is the angle in the $\mathbf{l}_0\mathbf{r}_0$-plane between the unit vector $\mathbf{l}_0$ and its projection $\mathbf{l}_c$ on the cone, see Fig. 4. The new unit vectors $\mathbf{l}_c$, $\mathbf{r}_c$ and $\mathbf{t}_c$, shown in Fig. 4, given by

$$\begin{bmatrix} \mathbf{l}_c \\ \mathbf{r}_c \\ \mathbf{t}_c \end{bmatrix} = \mathbf{A}_c^{\mathrm{T}} \begin{bmatrix} \mathbf{l}_0 \\ \mathbf{r}_0 \\ \mathbf{t}_0 \end{bmatrix} \tag{44}$$

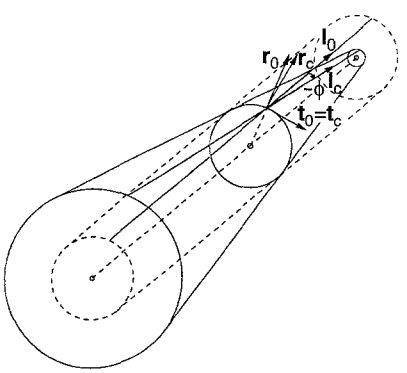

Fig. 4. The transformation due to the conical angle

where the orthogonal transformation matrix A_c is

$$\mathbf{A}_c = \begin{bmatrix} a_{l_c}^{l_0} & a_{r_c}^{l_0} & a_{t_c}^{l_0} \\ a_{l_c}^{r_0} & a_{r_c}^{r_0} & a_{t_c}^{r_0} \\ a_{l_c}^{t_0} & a_{r_c}^{t_0} & a_{t_c}^{t_0} \end{bmatrix} = \begin{bmatrix} \cos(\phi) & -\sin(\phi) & 0 \\ \sin(\phi) & \cos(\phi) & 0 \\ 0 & 0 & 1 \end{bmatrix} \tag{45}$$

The third step in the coordinate transformation is to take account of the spiral grain angle θ. This is performed in the same way as for the conical angle. The spiral grain angle is defined as the angle in the $\mathbf{l}_c\mathbf{t}_c$-plane between the unit vector $\mathbf{l}_c$ and the fibre direction $\mathbf{l}$, see Fig 5. The orthotropic unit vectors present following this transformation, denoted as $\mathbf{l}$, $\mathbf{r}$ and $\mathbf{t}$, are given by

$$\begin{bmatrix} \mathbf{l} \\ \mathbf{r} \\ \mathbf{t} \end{bmatrix} = \mathbf{A}_s^T \begin{bmatrix} \mathbf{l}_c \\ \mathbf{r}_c \\ \mathbf{t}_c \end{bmatrix} \tag{46}$$

where the orthogonal transformation matrix A_s is

$$\mathbf{A}_s = \begin{bmatrix} a_l^{l_c} & a_r^{l_c} & a_t^{l_c} \\ a_l^{r_c} & a_r^{r_c} & a_t^{r_c} \\ a_l^{t_c} & a_r^{t_c} & a_t^{t_c} \end{bmatrix} = \begin{bmatrix} \cos(\theta) & 0 & \sin(\theta) \\ 0 & 1 & 0 \\ -\sin(\theta) & 0 & \cos(\theta) \end{bmatrix} \tag{47}$$

This allows the relation between the local and the global coordinate systems to be expressed as

$$\begin{bmatrix} \mathbf{l} \\ \mathbf{r} \\ \mathbf{t} \end{bmatrix} = \mathbf{A}^T \begin{bmatrix} \mathbf{i} \\ \mathbf{j} \\ \mathbf{k} \end{bmatrix} \tag{48}$$

where

$$\mathbf{A} = \begin{bmatrix} a_l^x & a_r^x & a_t^x \\ a_l^y & a_r^y & a_t^y \\ a_l^z & a_r^z & a_t^z \end{bmatrix} = \mathbf{A}_0\mathbf{A}_c\mathbf{A}_s \tag{49}$$

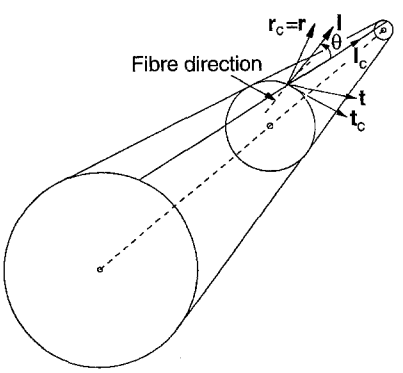

Fig. 5. The transformation due to the spiral grain angle

in which a_{local}^{global} denotes the direction cosines between the local and the global directions, respectively, see Fig. 2. This, in turn, allows the material relation in the global coordinate system to be expressed as

$$\dot{\boldsymbol{\sigma}} = \mathbf{D}\dot{\boldsymbol{\varepsilon}} - \dot{\boldsymbol{\sigma}}_0 \tag{50}$$

where

$$\dot{\boldsymbol{\sigma}} = \mathbf{G}^T\dot{\bar{\boldsymbol{\sigma}}} \tag{51}$$

$$\dot{\boldsymbol{\sigma}}_0 = \mathbf{G}^T\dot{\bar{\boldsymbol{\sigma}}}_0 \tag{52}$$

$$\dot{\bar{\boldsymbol{\varepsilon}}} = \mathbf{G}\dot{\boldsymbol{\varepsilon}} \tag{53}$$

$$\mathbf{D} = \mathbf{G}^T\bar{\mathbf{D}}\mathbf{G} \tag{54}$$

where a bar over the letter denotes the local coordinate system and **G** is a transformation matrix given by

$$\mathbf{G} = \begin{bmatrix} a_l^x a_l^x & a_l^y a_l^y & a_l^z a_l^z & a_l^x a_l^y & a_l^z a_l^x & a_l^y a_l^z \\ a_r^x a_r^x & a_r^y a_r^y & a_r^z a_r^z & a_r^x a_r^y & a_r^z a_r^x & a_r^y a_r^z \\ a_t^x a_t^x & a_t^y a_t^y & a_t^z a_t^z & a_t^x a_t^y & a_t^z a_t^x & a_t^y a_t^z \\ 2a_l^x a_r^x & 2a_l^y a_r^y & 2a_l^z a_r^z & a_l^x a_r^y + a_l^y a_r^x & a_l^z a_r^x + a_l^x a_r^z & a_l^y a_r^z + a_l^z a_r^y \\ 2a_t^x a_l^x & 2a_t^y a_l^y & 2a_t^z a_l^z & a_t^x a_l^y + a_t^y a_l^x & a_t^z a_l^x + a_t^x a_l^z & a_t^y a_l^z + a_t^z a_l^y \\ 2a_r^x a_t^x & 2a_r^y a_t^y & 2a_r^z a_t^z & a_r^x a_t^y + a_r^y a_t^x & a_r^z a_t^x + a_r^x a_t^z & a_r^y a_t^z + a_r^z a_t^y \end{bmatrix} \tag{55}$$

The matrix **G** includes the direction cosines given in Eq. (49).

Finite element formulation

A finite element formulation for simulating deformations and stresses in wood during moisture variation is given by

$$\mathbf{K}\dot{\mathbf{a}} = \dot{\mathbf{P}} + \dot{\mathbf{P}}_0 \tag{56}$$

where $\dot{\mathbf{a}}$ is the rate of nodal displacement and the other matrices are given by

$$\mathbf{K} = \int_V \mathbf{B}^T\mathbf{D}\mathbf{B}\,dV \tag{57}$$

$$\dot{\mathbf{P}} = \int_S \mathbf{N}^T\dot{\mathbf{t}}\,dS + \int_V \mathbf{N}^T\dot{\mathbf{f}}\,dV \tag{58}$$

$$\dot{\mathbf{P}}_0 = \int_V \mathbf{B}^T\dot{\boldsymbol{\sigma}}_0\,dV \tag{59}$$

where **K** is the stiffness matrix, the vector $\dot{\mathbf{P}}$ represents the load due to the boundary force vector $\dot{\mathbf{t}}$ and the body force vector $\dot{\mathbf{f}}$ and the vector $\dot{\mathbf{P}}_0$ includes the pseudo-load due to change in moisture content. The matrices **N** and **B** express the

shape functions and the strain shape functions, respectively, for the type of element employed. Since Eq. (56) is nonlinear, the global displacement vector **a** must be determined using a numerical time-stepping procedure. A number of different numerical procedures are available to use, see e.g. (Zienkiewicz and Taylor 1991). Numerical results obtained using the formulation described in the present paper are dealt with in (Ormarsson et. al 1998a, 1998b).

Conclusions

A three-dimensional theory for the numerical simulation of deformations in wood during moisture variations is described here. A finite element formulation is used to describe the deformation process and stress development. Wood is assumed to be a strongly orthotropic material. The total strain rate is assumed to be the sum of the elastic strain rate, the moisture-induced strain rate and the mechano-sorption strain rate. The material properties are assumed to be influenced by moisture content and by temperature. The model takes account of the influence which the growth rings, the spiral grain and the conical shape of the log have on the orthotropic directions in the wood.

References

Bodig J, Jayne BA (1982) Mechanics of wood and wood composites, Van Nostrand Reinhold Company, New York

Carlsson H, Thunell B (1975) Shrinking behaviour of wood during drying effect of tensile stresses, Paperi ja Puu, No., 7

Castera P (1989) Tensile creep of small wood specimens across the grain under drying conditions, Proc. of the IUFRO Int. Wood Drying Symp., Seattle

Dinwoodie JM (1981) Timber, its nature and behaviour, Van Nostrand Reinhold Company, New York

Johansson G, Kliger IR, Perstorper M (1994) Quality of structural timber-product specification system required by end-users, Holz Roh- Werkstoff 52(1):

Kollmann FFP, Côté Jr., WA (1968) Principles of Wood Science and Technology. I. Solid Wood, Springer-Verlag, Berlin

Ormarsson S, Dahlblom O, Petersson H (1998a) Numerical Study of Shape Stability of Sawn Timber Subjected to Moisture Variations, Part 2: Simulation of Drying Board, to appear in Wood Sci and Technol

Ormarsson S, Dahlblom O, Petersson H (1998b) Numerical Study of Shape Stability of Sawn Timber Subjected to Moisture Variations, Part 3: Influence of Annual Ring Orientation, to appear in Wood Sci and Technol

Perstorper M, Pellicane PJ, Kliger IR, Johansson G (1995) Quality of timer products from Norway spruce, Part 1: Quality optimization, key variables and experimental study, Wood Sci Technol: 157–171

Ranta-Maunus A (1990) Impact of mechano-sorption creep to the long-term strength of timber, Holz Roh- Werkstoff: 67–71

Santaoja K, Leino T, Ranta-Maunus A, Hanhijärvi A (1991) Mechano-sorptive structural analysis of wood by the ABAQUS finite element program, Technical Research Centre of Finland, Research notes 1276, Espoo

Thelandersson S, Morén T (1990) Tensile stresses and cracking in drying timber, IUFRO/5.02 Timber Engineering Meeting, New Brunswick

Zienkiewicz OC, Taylor RL (1991) The Finite Element Method, forth edition, Vol. 2, McGraw-Hill, London